Original Article

miR-99 family is potential target to reverse cerium dioxide nanoparticle-induced placental cell dysfunction

Mengmeng Yao[1,2#], Xiaoli Ji[1#], Yuqing Zhang[2], Zhilei Mao[3], Xia Chi[1,2]

[1]Institute of Toxicology, School of Public Health, Nanjing Medical University, Nanjing, China; [2]Department of Child Health Care, Women's Hospital of Nanjing Medical University, Nanjing Maternity and Child Health Care Hospital, Nanjing, China; [3]Department of Child Health Care, Changzhou Maternal and Child Health Care Hospital, Changzhou, China

Contributions: (I) Conception and design: M Yao; (II) Administrative support: X Chi, Z Mao; (III) Provision of study materials: X Ji; (IV) Collection and assembly of data: Y Zhang; (V) Data analysis and interpretation: M Yao; (VI) Manuscript writing: All authors; (VII) Final approval of manuscript: All authors.

[#]These authors contributed equally to this work.

Correspondence to: Zhilei Mao. Department of Child Health Care, Changzhou Maternal and Child Health Care Hospital, No. 16 Dingxiang Road, Changzhou 213000, China. Email: mao598808386@126.com; Xia Chi, PhD. Department of Child Health Care, Women's Hospital of Nanjing Medical University, Nanjing Maternity and Child Health Care Hospital, No. 123 Tianfei Lane, Mochou Road, Nanjing 210004, China. Email: chixia2001@njmu.edu.cn.

Background: Cerium dioxide nanoparticles (CeO_2 NPs) are increasingly used as diesel additive, causing a lot of concern about their toxic effects when released into the atmosphere. To date, there is little knowledge about the toxic effects of CeO_2 NPs on the female reproductive system.

Methods: The morphology and size distribution of CeO_2 NPs was observed by transmission electronic microscope (TEM) and Zetasizer Nano, respectively. The uptake of CeO_2 NPs by cells was also observed by TEM after treatment. The cytotoxicity of CeO_2 NPs was studied by Cell Counting Kit-8 (CCK-8), the cellular invasive and migratory ability was examined by transwell assay, the cell apoptosis and reactive oxygen species (ROS) were studied by flow cytometry (FCM), and the mRNAs and proteins expressions were revealed by quantitative real-time PCR (qRT-PCR) and western blotting. The cytoskeletons and autophagy levels were revealed by immunofluorescence. The target regulation of miR-99 to mammalian target of rapamycin (mTOR) was proved by dual luciferase reporter assay after transfection.

Results: We studied the cytotoxic effects of CeO_2 NPs on human trophoblastic cells (HTR-8/Svneo) and found that the invasive and migratory abilities of HTR-8/SVneo cells were decreased after CeO_2 NPs exposure. Immunofluorescence assays showed that the cellular microtubule networks and microfilament arrangement were obviously altered, and although the expression of cytoskeleton proteins (α-tubulin, β-tubulin, actin) did not change, the protein levels of invasion- and migration-related factors [matrix metalloproteinase 2 (MMP2), protein kinases B (AKT), mTOR] were decreased in exposed cells. Accordingly, the expression level of miR-99 family members (miR-99a, miR-99b, miR-100), which can regulate mTOR, was significantly increased after CeO_2 NPs exposure. Dual luciferase reporter assay indicated that the miR-99 family members directly targeted mTOR.

Conclusions: CeO_2 NPs impaired the invasive and migratory abilities, which play an important role in embryo implantation, as well as determining placental function and embryonic development.

Keywords: Cerium dioxide nanoparticles (CeO_2 NPs); invasion and migration; mammalian target of rapamycin (mTOR); miR-99 family; trophoblast cells

Submitted Dec 30, 2021. Accepted for publication Mar 07, 2022.
doi: 10.21037/atm-22-508
View this article at: https://dx.doi.org/10.21037/atm-22-508

Introduction

The application of nanomaterials in industry, food, medicine, cosmetics and other fields is increasing rapidly (1), and many are released into the environment eventually, which may bring potential health and environmental risks (2). Owing to their excellent physicochemical properties, cerium dioxide nanoparticles (CeO_2 NPs) are extensively used in ultraviolet absorbents, solar cells, catalysts, gas sensing, and precision instrumental glass polishing (3-5). Ce-based fuel-borne catalysts can improve fuel-burning efficiency and decrease exhaust emission of green-house gases and particle numbers (6,7). However, CeO_2 NPs themselves would be emitted with the vehicle exhaust into the atmosphere and be potentially hazardous for human health (8). To date, no evidence suggested the current CeO_2 NPs concentrations in the atmosphere, and the population exposure data is lacking, so the adverse effects should be studied firstly in animal or cell models to speculate their potential risks.

NPs can easily penetrate damaged skin, or enter the body via lungs or the gut (9-11) due to their small size. They can even penetrate the placental barrier and impair placental functions (12,13). For instance, nanosilica particles can generate reactive oxygen species (ROS) and induce placental inflammation, resulting in pregnancy complications (14); polyethylene glycol-single-walled carbon nanotubes reportedly had teratogenic effects in mice (15); and in another mouse model, after maternal exposure to carbon-black NPs, the mRNA expressions of genes related to angiogenesis, cell migration, chemotaxis and growth factor production were altered in the cerebral cortex of the offspring (16). Some studies had reported that exposure to CeO_2 NPs can induce inflammation, ROS, cell apoptosis and autophagy (17-19). In addition, short terms exposure of CeO_2 NPs to ram sperm induces no significant adverse effects (20), while chronic exposure decreased the mice testis weight, sperm motility and increased the abnormal gene expressions (21). While a previous study indicated that low concentration of CeO_2 NPs enhanced embryo production of prepubertal ovine oocytes *in vitro* (22), the current little evidence suggested the effects of CeO_2 NPs on reproductive system need to be further studied. Our previous population study found that the Ce element level in the placenta of patients with spontaneous abortion was higher than in normal pregnant women (unpublished data), but the effects of CeO_2 NPs on trophoblast cells are unknown. In the current study, we used HTR-8/SVneo cells as a good cell model for mechanical exploration (23), mainly focusing on invasive ability, which is extremely important for trophoblast development. We present the following article in accordance with the MDAR reporting checklist (available at https://atm.amegroups.com/article/view/10.21037/atm-22-508/rc).

Methods

Characterization of CeO_2 NPs

CeO_2 NPs (product No. YFO07-N50) were purchased from XFNANO, Inc. (Shanghai, China). Their morphology was observed by transmission electron microscopy (TEM) (JEOL JEM 2100) after the CeO_2 NPs were added to double-distilled H_2O (ddH_2O), vortex mixed at high speed for 1 min. Particle size distribution of CeO_2 NPs in complete cell culture medium was determined by Zetasizer Nano (ZS90, UK).

Cell culture and treatment with CeO_2 NPs

HTR-8/SVneo cells, purchased from American Type Culture Collection (CRL-3271), originated from human placental trophoblasts. The cells were cultured with RPMI-1640 cell culture medium supplemented with 10% fetal bovine serum (FBS), 100 U/mL penicillin and 100 μg/mL streptomycin at 37 ℃ under 5% CO_2 culture conditions. After the cells reached 60% confluence, CeO_2 NPs were administered at the indicated concentrations (0, 1, 10, 100 μg/mL) and incubated for 24 h.

Uptake analysis

The localization of CeO_2 NPs in HTR-8/SVneo cells was observed by TEM. Briefly, cells were administered 100 μg/mL of CeO_2 NPs for 24 h. After washing twice with phosphate-buffered saline (PBS), the cells were collected and fixed with glutaraldehyde (2%). Osmium tetroxide buffer (1%) was used for post-fixation, and a graded acetone series was applied for dehydration. After being embedded in araldite, samples were cut into ultrathin slices and observed under TEM.

Cell viability analysis

Cell viability was evaluated with a Cell Counting Kit-8 (CCK-8) Assay Kit (Dojindo, Japan) according to the

manufacturer's protocol. Briefly, cells were seeded in a 96-well plate at the correct density per well and treated with a range of concentrations of CeO_2 NPs (0, 1, 10, 100 μg/mL) for 24 h. Next, 10 μL CCK-8 solution was added to each well, and the plates were incubated for another 1–4 h. The supernatant was removed to another 96-well plate, and absorbance was determined at 450 nm with a UV/vis spectrometer (Ocean Optics, HR4000).

Analysis of ROS

Flow cytometry (FCM) was used to detect ROS using a Reactive Oxygen Species Assay Kit (Beyotime, China). After 24-h treatment with CeO_2 NPs, cells were trypsinized, centrifuged at 100g for 3 min, and incubated with 2,7-dichlorodi-hydrofluorescein diacetate for 30 min, then washed three times with PBS. Finally, the stained cells were collected for FCM analyses at 488 nm excitation.

Cell apoptosis assay

Annexin V apoptosis detection kit (BD Pharmingen, USA) was used to detect the levels of cell apoptosis. After CeO_2 NP treatment, cells were collected and washed three times with PBS. Appropriate numbers of cells were incubated in 100 μL of 1× binding buffer together with 5 μL fluorescein isothiocyanate (FITC)-Annexin V and 5 μL propidium iodide (PI) for 15 min at room temperature in the dark. Next, 400 μL of 1× binding buffer was added and the cell suspension was mixed and measured with FCM.

Matrigel invasion assay

An invasion assay of HTR-8/SVneo cells was evaluated by transwell assay (8-μm pore size; Costar, Cambridge, UK). Briefly, cells were seeded in 6-well plates and treated with CeO_2 NPs for 24 h, then 2×10^5 cells were resuspended in 100 μL serum-free medium and plated in the upper chamber, which was coated with Matrigel, and 700 μL RPMI 1640 medium supplied with 10% FBS was added to the lower well and plates were incubated for 24 h. Cells that invaded through the membrane filter were fixed with methanol and stained with crystal violet. Images were obtained with a Nikon light microscope at 100× magnification.

Immunofluorescence microscopy

Cellular cytoskeletons were observed with a confocal microscope after immunofluorescence. Cells were seeded in glass bottom dishes (NEST, 801001) at the correct density and cultured overnight, after which the cells were treated with 100 μg/mL CeO_2 NPs for another 24 h. After removal of the culture medium, cells were then fixed with 4% paraformaldehyde for 30 min. Microtubules was revealed by anti-β-tubule antibody (Abcam, ab52623), combined with FITC-conjugated secondary goat antibody (Beyotime, A0562, A0568). Microfilaments were revealed with rhodamine phalloidin (Sigma, 1:200). Autophagy was revealed by anti-LC3A/B antibody (CST, #4108), and CY3 conjugated secondary antibody. Cell nuclei stained blue with 4',6-diamidino-2-phenylindole (DAPI) (Beyotime, C1006). Images were obtained with a confocal microscope at 100× objective lens amplification (Nikon, Japan).

Western blotting analysis

Western blotting analysis was used to determine the protein expression levels. HTR-8/SVneo Cells were seeded and treated with CeO_2 NPs for another 24 h, and when incubation finished, the cells were lysed using RIPA, containing phenylmethyl sulfonyl fluoride (PMSF), for subsequent protein extraction. The BCA Protein Assay Kit (Beyotime, China) was used to examine the protein concentrations in each sample. 80 μg of the total proteins were loaded to 10% SDS-PAGE for electrophoresis. The antibodies of α-tubulin (Beyotime, AF5012), β-tubulin (Beyotime, AF1216), actin (Beyotime, AA128), protein kinases B (AKT) (CST, #9272), mammalian target of rapamycin (mTOR) (CST, #2972), matrix metalloproteinase 2 (MMP2) (Abcam, ab92536), MMP9 (Abcam, ab76003), and LC3A/B (CST, #4108) were used to quantify the protein levels, and glyceraldehyde 3-phosphate dehydrogenase (GAPDH) (Beyotime, AF5009) was used as the loading control. Immunoblots were visualized with an enhanced chemiluminescence (ECL) western blot detection kit (Millipore) combined with the Bio-Rad Imaging System. All experiments were repeated at least three times.

RNA isolation and quantitative real-time PCR (qRT-PCR) assay

Total RNA extraction was performed using TRIzol reagent (Invitrogen, Carlsbad, CA, USA) according to the manufacturer's instructions, and the concentration of total RNA was determined using Nano Drop 2000 (Thermo Fisher Scientific, Waltham, MA, USA) at the absorbance

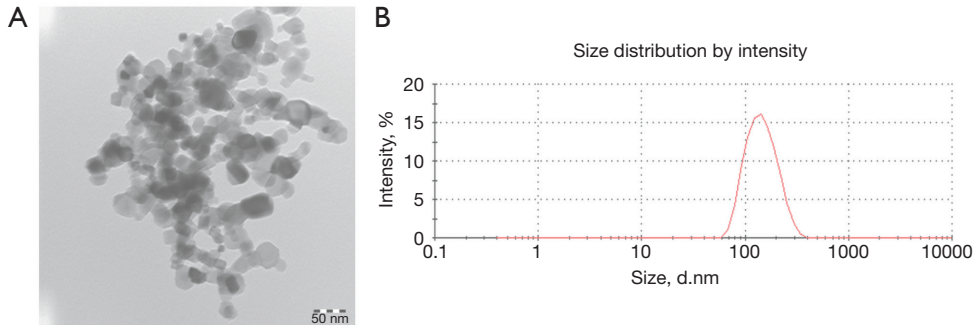

Figure 1 The characteristics of CeO_2 NPs. (A) TEM image of CeO_2 NPs. Scale bar =50 nm. (B) The dynamic light scattering results of the hydrodynamic size distribution of CeO_2 NPs in complete cell culture medium (RPMI-1640). CeO_2 NPs, cerium dioxide nanoparticles; TEM, transmission electron microscopy.

of 260 nm. cDNA and miRNA were prepared according to the Mir-X™ miRNA qRT-PCR TB Green® kit instructions (Takara, Tokyo, Japan). RT-PCR was performed using SYBR PCR Master Mix reagent kits (Takara, Tokyo, Japan) in an ABI 7900 Fast Real-Time System (Applied Biosystems, Foster City, CA, USA). All primers were synthesized by Invitrogen, Shanghai, China. All assays were independently repeated at least three times.

Bioinformatics: predicting potential miRNAs, mRNA

The following three databases were used to predict miRNAs targeting mTOR: miRanda (https://www.cbio.mskcc.org/mirnaviewer/), TargetScan (http://www.targetscan.org) and RNA22 (https://cm.jefferson.edu/rna22/). Intersection miRNAs were chosen for the following study.

miRNA transfection and luciferase reporter assay

The mimics and inhibitors of miR-99 family members (miR-99a, miR-99b, miR-100) and a negative control (NC) were chemically synthesized by GenePharma (Shanghai, China). HTR-8/SVneo cells were plated in 6-well plates at 50% confluence and transfection was carried out using Lipofectamine 2000 (Invitrogen, Carlsbad, USA). Total RNA or proteins were collected at 24 h post-transfection. For the luciferase reporter assay, the cells were plated into 24-well plates and co-transfected with luciferase reporter vectors and 50 nM mimic/control respectively using Lipofectamine 2000. The Renilla luciferase vector pRL-SV40 (5 ng) was used for normalization. After 24 h, the luciferase activity was measured with the Dual-Luciferase Reporter System according to the manufacturer's protocols (Promega, Madison, USA). Firefly luciferase activity was normalized to Renilla luciferase activity.

Statistical analysis

All experiments were replicated at least three times, and all the data are presented as mean ± standard error (SE) from three independent assays. Statistical analysis was performed using STATA9.2, and one-way analysis of variance (ANOVA) followed by Dunnet's test was used to determine the differences between the control and CeO_2 NPs treatment groups. $P<0.05$ was considered significant.

Results

Characterization of CeO_2 NPs

The TEM images showed that CeO_2 NPs were nearly spherical with an average primary diameter of 45.9±8.9 (range, 25.5–79.8) nm (*Figure 1A*). The dynamic light scattering results showed that CeO_2 NPs slightly aggregated in the culture medium with a poly dispersion index of 0.128. The particle size distribution (*Figure 1B*) demonstrated that the hydrodynamic diameter of CeO_2 NPs was 137.7± 51.56 nm in culture medium, and the result quality was good.

General toxicity of CeO_2 NPs

Cells were treated with CeO_2 NPs (0, 1, 10, and 100 μg/mL) for 24 h, and cell viability was examined by CCK-8. *Figure 2A* shows that cell viability was not affected after exposure, and the morphology of HTR-8/SVneo cells showed no obvious change (*Figure 2B*). The results of FCM showed that CeO_2 NPs did not increase the production of

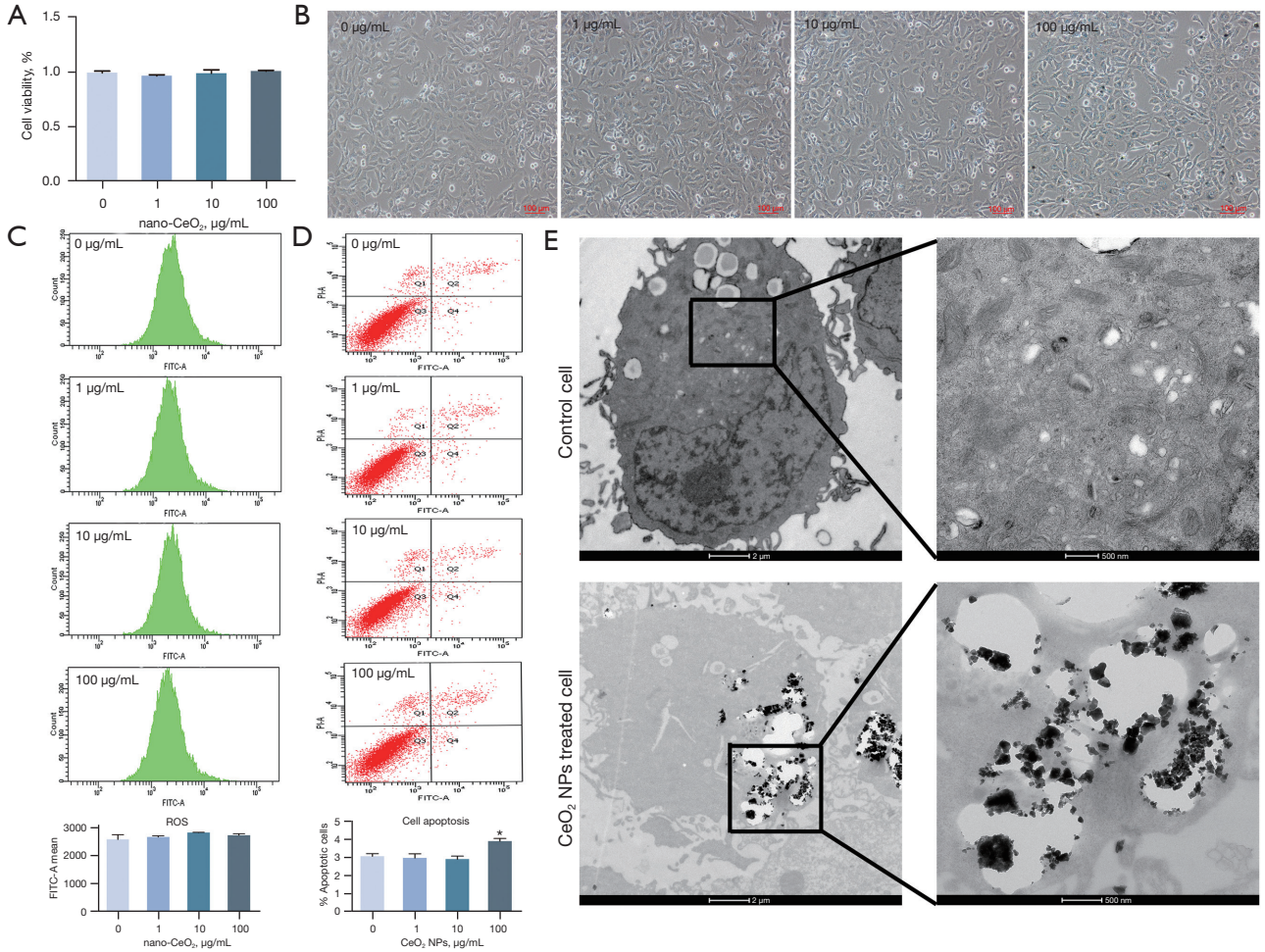

Figure 2 Effects of CeO_2 NPs on cell viability, ROS formation and cell apoptosis after taken in. (A) Viability of HTR-8/SVneo cells measured by CCK-8 assay kit after exposure to concentrations of CeO_2 NPs for 24 h. (B) Cell morphology observed by a light microscope at 100× magnification after cells were treated with different concentrations of CeO_2 NPs. Scale bar =100 μm. (C,D) ROS and apoptosis levels examined by FCM after CeO2 NPs treatment, all results obtained from three independent experiments, and presented as mean ± SE. (*P<0.05). (E) Uptake of CeO_2 NPs observed by TEM after the cells were treated with 100 μg/mL of CeO_2 NPs for 24 h. CeO_2 NPs in cytoplasm are indicated in the inset. Scale bar =2 μm, 500 nm. CeO_2 NPs, cerium dioxide nanoparticles; CCK-8, Cell Counting Kit-8; ROS, reactive oxygen species; FCM, flow cytometry; SE, standard error; TEM, transmission electron microscopy.

ROS (*Figure 2C*), and cell apoptosis showed an increasing but not significant trend at 100 μg/mL of CeO_2 NPs (*Figure 2D*). The TEM image (*Figure 2E*) showed that CeO_2 NPs were intracellular and mainly located in the cytoplasm.

Effect of CeO_2 NPs on the migratory and invasive abilities of HTR-8/SVneo cells

Matrigel invasion assay was used to study the influence of CeO_2 NPs on the invasive ability of HTR-8/SVneo cells, because invasion plays an important role in embryo implantation (24). The results showed that compared with the control group, the number of penetrated cells in the CeO_2 NPs-treated groups decreased significantly (P<0.05) (*Figure 3A*), indicating decreased invasive ability of HTR-8/SVneo cells after CeO_2 NPs exposure.

Effect of CeO_2 NPs on cellular cytoskeleton networks

The microtubules and microfilament have great significance in cell migration and invasion (25). To confirm whether CeO_2 NPs affected these networks, the

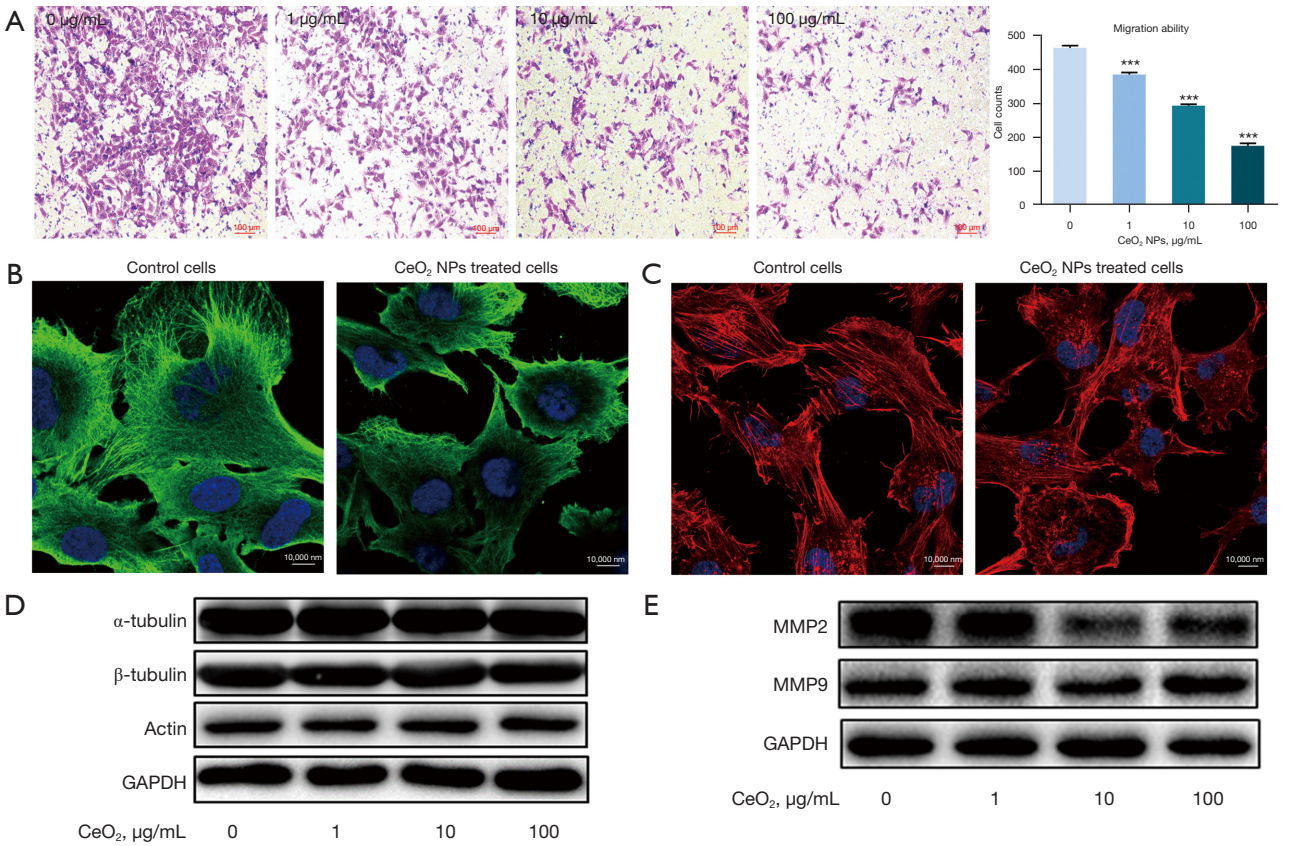

Figure 3 Adverse effects of CeO_2 NPs on cell migration and invasion ability and examination of affecting factors. (A) Transwell analysis of HTR-8/SVneo cells after CeO_2 NPs exposure. Cells were stained with crystal violet, imaged and counted under a Nikon light microscope. Five independent eyesights were selected to count the cells were counted and values were expressed as mean ± SE (***P<0.001). Scale bar =100 μm. (B) Microtubulular network of HTR-8/SVneo cells after treatment with 100 μg/mL CeO_2 NPs. The network was revealed with anti-β tubule and goat anti-rabbit IgG conjugated with FITC. Scale bar =10 μm. (C) Microfilament network of HTR-8/SVneo cells colored with rhodamine phalloidin. Scale bar =10 μm. (D,E) Western blot analysis of the expression of α-/β-tubule, actin, MMP2 and MMP9 proteins between control group and CeO_2 NPs treated groups. GAPDH acted as the loading control. CeO_2 NPs, cerium dioxide nanoparticles; GAPDH, glyceraldehyde 3-phosphate dehydrogenase; MMP, matrix metalloproteinase; SE, standard error; IgG, immunoglobulin G; FITC, fluorescein isothiocyanate.

cytoskeletons of HTR-8/SVneo cells were examined using immunofluorescence with α-tubule antibody and rhodamine phalloidin, respectively. As shown in *Figure 3B*, compared with the control group, the microtubule arrangement of CeO_2 NP-treated cells was disordered. Moreover, the density of microtubules appeared decreased. The microtubules failed to form long and extended networks, and the networks were remodeled in CeO_2 NP-treated cells. As for the microfilaments, actins formed long, straight stress fibers that ran parallel to the long axis and penetrated the cells in the control cell, whereas in CeO_2 NP-treated cells, the arrangement of stress fibers was disorganized, and some cells even lost their stress fibers (*Figure 3C*). In addition, we examined the protein expression level of the cytoskeleton (microtubules and microfilaments) by western blotting. The results showed that the expressions of α-tubulin, β-tubulin and actin were unchanged (*Figure 3D,3E*).

Effect of CeO_2 NPs on the expression of invasion-related proteins

Previous studies showed that the expression and activation of MMP2 and MMP9 can promote trophoblast invasion (26,27). To determine whether CeO_2 NP exposure affected

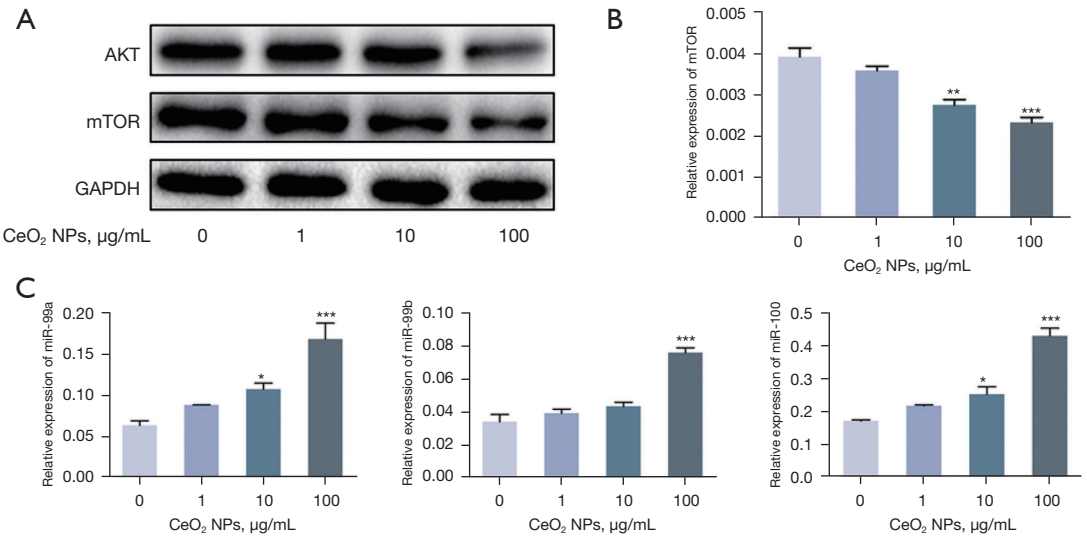

Figure 4 The expression of cell migration related factors and the target protein related microRNA expression. (A) AKT/mTOR protein levels determined by western blot. (B) mTOR mRNA level determined by qRT-PCR using a housekeeping gene GAPDH as an internal control. (C) Expression levels of miR-99 family members (miR-99a, miR-99b, miR-100) determined by qRT-PCR. *P<0.05; **P<0.01; ***P<0.001. AKT, protein kinases B; mTOR, mammalian target of rapamycin; GAPDH, glyceraldehyde 3-phosphate dehydrogenase; CeO_2 NPs, cerium dioxide nanoparticles; qRT-PCR, quantitative real-time PCR.

MMP production in trophoblasts, we examined the expressions of MMP2 and MMP9 in HTR-8/SVneo cells treated with CeO_2 NPs. As shown in *Figure 4A*, MMP2 expression was decreased, but the levels of MMP9 did not change.

Effect of CeO_2 NPs on the expression of migration-related factors

The PI3K/AKT/mTOR pathway plays crucial roles in cell growth, proliferation, survival, protein synthesis, transcription and cell migration (28-30). However, whether CeO_2 NPs can inhibit mTOR signaling has been unclear. We therefore assessed the expression of AKT and mTOR after CeO_2 NP treatment. The results showed that CeO_2 NPs significantly decreased the expression of mTOR at both the mRNA and protein levels (*Figure 4A*,*4B*). Meanwhile, the protein level of AKT was also decreased (*Figure 4A*). To explore the mechanisms by which CeO_2 NPs disturbed the expression of mTOR in HTR-8/SVneo cells, the related miRNAs were predicted, and the expressions of miR-99 family members were evaluated. We found that miR-99a/b and miR-100 were all increased after CeO_2 NP exposure (*Figure 4C*).

Target of miR-99 family in HTR-8/SVneo cells

After we confirmed the efficiency of transfection, the expression levels of miR-99 family members, and the mRNA and protein levels of mTOR were also measured after the inhibitor/NC precursor was transfected for 24 h. The results showed that the relative expression levels of the miR-99 family members were decreased by miR-99 family inhibitor in HTR-8/SVneo cells (*Figure 5A*). As expected, the mRNA and protein levels of mTOR were increased with miR-99 family inhibitor (*Figure 5B-5D*). To investigate whether miR-99 family members directly bind to the 3'untranslated region (UTR) of mTOR, we performed miRNA dual luciferase reporter assay by constructing wild-type and mutant-type luciferase reporter plasmids containing the binding region of the 3'UTR of mTOR mRNA. We found that co-transfection of miR-99 family member mimics and pGL3-mTOR-miR-99a/99b/100-WT reporter plasmids significantly decreased the luciferase activity in HTR-8/SVneo cells, as compared with the control (*Figure 5E*). These results suggested that the miR-

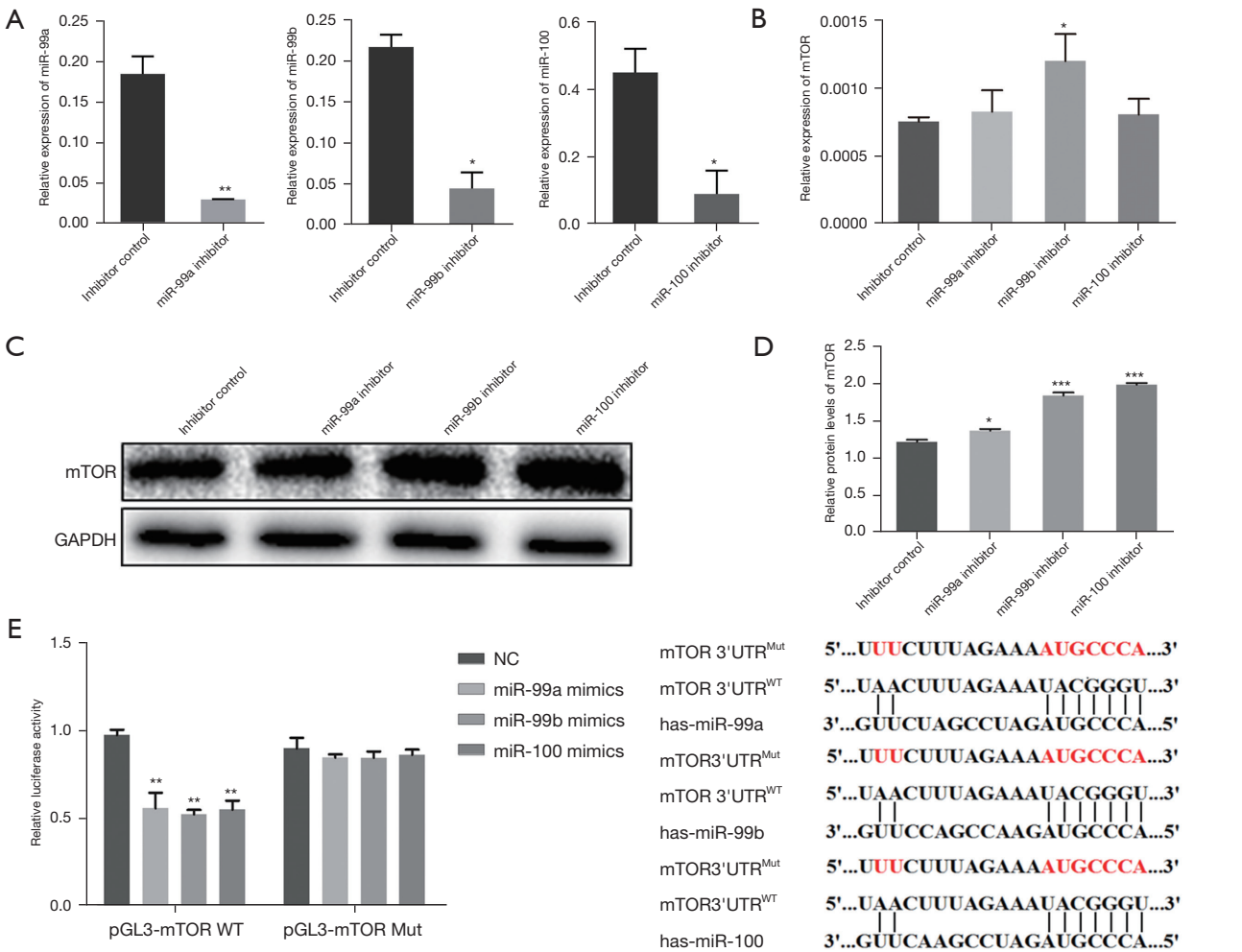

Figure 5 Verification of the target regulation of miR-99 family on mTOR. (A) qRT-PCR performed to evaluate the expression levels of miR-99 family members. Cells were transfected with 100 nM inhibitor or NC for 24 h. (B) Relative mRNA expression levels of mTOR after corresponding transfection. (C,D) Protein levels of mTOR after transfection. (E) Cells co-transfected with miR-99a/99b/100 mimics or control, Renilla luciferase vector pRL-SV40 and mTOR 3'UTR luciferase reporters for 24 h. Reporter activity was significantly decreased after miR-99a/99b/100 overexpression compared with control. Schematic representation of mTOR 3'UTR showing putative miR-99a/99b/100 target sites. *P<0.05; **P<0.01; ***P<0.001. mTOR, mammalian target of rapamycin; GAPDH, glyceraldehyde 3-phosphate dehydrogenase; NC, negative control; UTR, untranslated region; qRT-PCR, quantitative real-time PCR.

99 family directly targets mTOR.

Effect of miR-99 family inhibitor on the attenuation of trophoblast cells' invasive and migratory abilities by CeO_2 NPs exposure

To evaluate the effects of the miR-99 family on CeO_2 NP-induced impairment of trophoblast cells invasive ability, the corresponding inhibitors were added to reverse miR-99 family members. The results showed that CeO_2 NPs significantly impaired the invasive ability of HTR-8/SVneo cells, and when the inhibitors of miR-99 family members were added, the impairment of the cellular invasive and migratory abilities were partly reversed (*Figure 6A,6B*). Meanwhile, when the mTOR expressions were recovered after exposure to CeO_2 NPs (*Figure 6C,6D*), cell autophagy, which was mostly regulated by mTOR, was also rescued (*Figure 6E*).

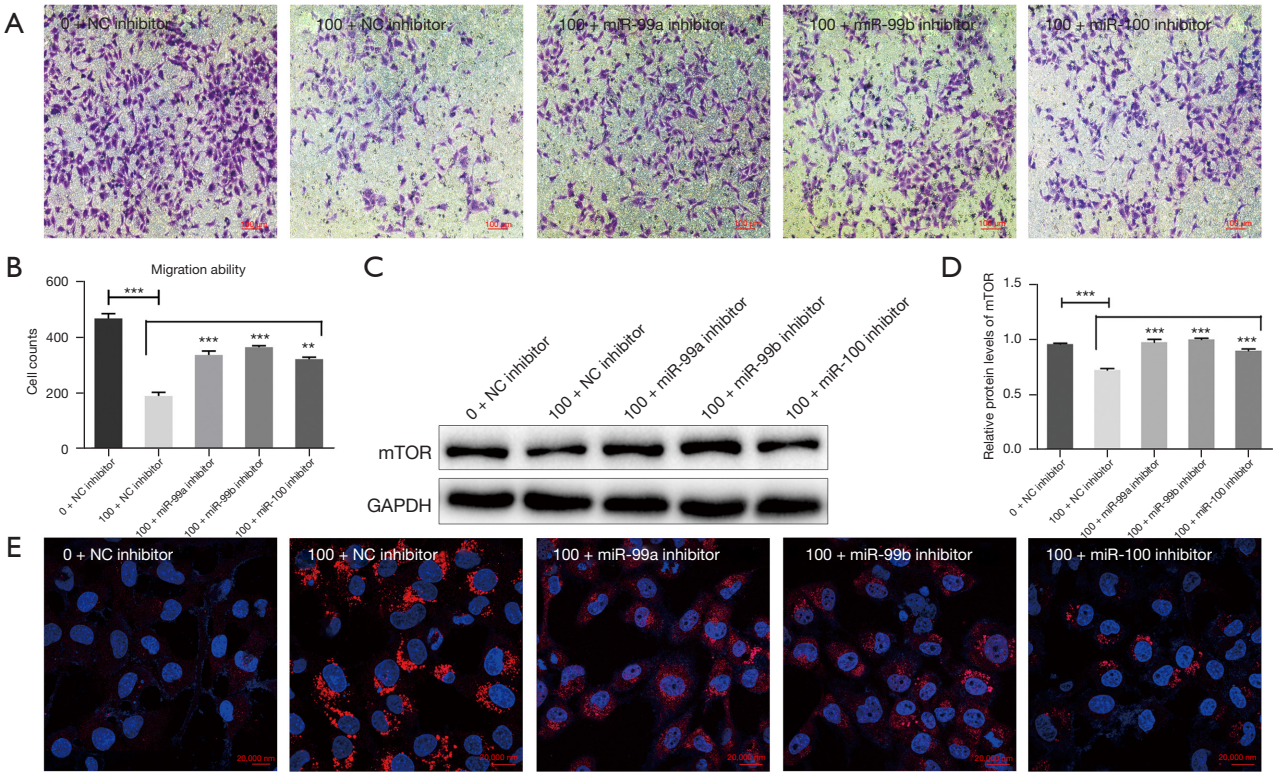

Figure 6 The reversal effects of miR-99 family on cell migration and invasion ability. (A,B) Transwell analysis showing the invasive and migratory abilities of HTR-8/SVneo cells after CeO_2 NPs exposure and following reversal with the inhibitors of miR-99 family members. Cells were stained with crystal violet, imaged and counted under a Nikon light microscope. Scale bar =100 μm. (C,D) Protein and mRNA levels of mTOR after treatment with CeO_2 NPs and transfected with miR-99 family members inhibitors. Each data point represented as mean ± SE from three independent experiments. **P<0.01; ***P<0.001. (E) Immunofluorescence results showing the autophagy levels revealed by LC3 antibody after cells were treated with CeO_2 NPs and miR-99 family inhibitors. The nuclei are stained blue with DAPI. Scale bar =50 μm. NC, negative control; mTOR, mammalian target of rapamycin; GAPDH, glyceraldehyde 3-phosphate dehydrogenase; CeO_2 NPs, cerium dioxide nanoparticles; SE, standard error; DAPI, 4',6-diamidino-2-phenylindole.

Discussion

The human placenta is functionally simultaneous with the development of maternal and embryonic fetal compartments. During development of the placenta, extravillous trophoblasts (EVTs), which differentiate from trophoblast cells, invade and remodel the uterine endometrium and maternal spiral arteries under the regulation of complex networks, such as cell types, mediators, and signaling pathways (31,32). Normal trophoblastic invasion and migration play an important role in the embryo obtaining sufficient nutrition and oxygen before vasculogenesis.

Several investigators have established trophoblast cell lines derived from first trimester placentae, which are commonly used to study trophoblast invasion and migration, such as HTR-8/SVneo (23). Although trophoblastic cells are a type of normal cell, they share several common features with malignant cells (33).

Previous study report that different types of NPs, such as gold NPs (34), and zinc sulfide NPs (35), can suppress migration/invasion by cancer cells, so some NPs could also inhibit the invasion and migration of HTR-8/SVneo cells. Whether CeO_2 NPs would impair the invasive and migratory abilities of HTR-8/SVneo cells, and what adverse effects that would have on human placental development have been unknown. Our results showed that CeO_2 NPs could impair these abilities of HTR-8/SVneo cells, but the mechanism remains unclear and requires further investigation.

Previous studies confirmed that trophoblast cells constitutively produce MMP2 and MMP9 and are strongly localized to the placental bed in early pregnancy and invasive by nature (36,37). In our study, the MMP2 protein levels decreased in the CeO_2 NP groups compared with the control group. Our results indicated that the CeO_2 NPs inhibition of the invasion of HTR-8/SVneo cells might be caused by changes in the MMPs. Studies have reported that the AKT pathway is involved in trophoblast invasion through promotion of MMP2 and MMP9 secretion (38,39). Another study reported that the PI3K/AKT/mTOR signaling pathway is generally regarded as a major regulator of migration (40). However, whether the CeO_2 NP-induced impairment of cellular invasion and migration was related to the PI3K/AKT/mTOR signaling pathway was unclear. We therefore assessed the expression of AKT and mTOR after CeO_2 NP treatment and our results suggested that mTOR signaling was inhibited after the treatment.

Recently, miRNAs have been considered as a new layer for gene and protein regulation, and are thought to be functionally important in influencing the different facets of trophoblast biology, such as proliferation, differentiation, syncytialization, and invasion (41). Previous studies indicated that miRNAs control the expression of invasion factors (42-44). In this study, mTOR was detected as decreased after exposed to CeO_2 NPs, and combining three bioinformatics software, we predicted that miR-99 family members might be the potential miRNAs targeting mTOR. Recent studies suggest that the miR-99 family members (miR-99a/b and miR-100) regulate cell migration and cell proliferation in several types of cancer of epithelial origin (45-47). In this study, we identified that miR-99 family members regulated the expression of mTOR in HTR-8/SVneo cells, and then confirmed their specific target sites by transfection and dual luciferase reporter assay, which provided a new insight into CeO_2 NP-inhibited invasion.

Briefly, this is the first report of CeO_2 NPs affecting the invasive and migratory abilities of trophoblastic cells by decreasing the expression of MMP2 and mTOR. The miR-99 family was the target for reversing the effects of the NPs in HTR-8/SVneo cells, which hinted at an adverse effect on embryo implantation and development, as well as provides a therapeutic pathway to overcome the effects of CeO_2 NPs.

Conclusions

Our study revealed that CeO_2 NPs could impair the invasive ability of HTR-8/SVneo cells by disturbing cytoskeletal arrangement, and decreasing the expressions of MMP2 and mTOR. The miR-99 family members (miR-99a/b and miR-100) could directly target mTOR, and downregulating the miR-99 family could rescue the cell invasion ability as well as mTOR expression. These findings suggested that CeO_2 NPs have potential risks for placental development via disturbance of normal trophoblast invasion and migration.

Acknowledgments

Funding: The study was supported by the National Natural Science Fund of China (No. 81703256); the Youth Talent Support Project of Changzhou Science and Technology Association; the Youth Talent Support Project of Jiangsu provincial Science and Technology Association; the Society Development Project of Changzhou Science and Technology Bureau (No. CE20215037, No. CJ20190032).

Footnote

Reporting Checklist: The authors have completed the MDAR reporting checklist. Available at https://atm.amegroups.com/article/view/10.21037/atm-22-508/rc

Data Sharing Statement: Available at https://atm.amegroups.com/article/view/10.21037/atm-22-508/dss

Conflicts of Interest: All authors have completed the ICMJE uniform disclosure form (available at https://atm.amegroups.com/article/view/10.21037/atm-22-508/coif). The authors have no conflicts of interest to declare.

Ethical Statement: The authors are accountable for all aspects of the work in ensuring that questions related to the accuracy or integrity of any part of the work are appropriately investigated and resolved.

References

1. Kessler R. Engineered nanoparticles in consumer products: understanding a new ingredient. Environ Health Perspect 2011;119:a120-5.
2. Nel A, Xia T, Mädler L, et al. Toxic potential of materials at the nanolevel. Science 2006;311:622-7.
3. Yu JC, Zhang L, Lin J. Direct sonochemical preparation of high-surface-area nanoporous ceria and ceria-zirconia solid solutions. J Colloid Interface Sci 2003;260:240-3.
4. Khan SB, Faisal M, Rahman MM, et al. Exploration of CeO_2 nanoparticles as a chemi-sensor and photo-catalyst for environmental applications. Sci Total Environ 2011;409:2987-92.
5. Corma A, Atienzar P, García H, et al. Hierarchically mesostructured doped CeO2 with potential for solar-cell use. Nat Mater 2004;3:394-7.
6. Selvan VAM, Anand RB, Udayakumar M. Effects of cerium oxide nanoparticle addition in diesel and diesel-biodiesel-ethanol blends on the performance and emission characteristics of a CI engine. J Eng Appl Sci 2009;4:1819-6608.
7. Logothetidis S, Patsalas P, Charitidis C. Enhanced catalytic activity of nanostructured cerium oxide films. Materials Science and Engineering: C 2003;23:803-6.
8. Cassee FR, Campbell A, Boere AJ, et al. The biological effects of subacute inhalation of diesel exhaust following addition of cerium oxide nanoparticles in atherosclerosis-prone mice. Environ Res 2012;115:1-10.
9. Leite-Silva VR, Le Lamer M, Sanchez WY, et al. The effect of formulation on the penetration of coated and uncoated zinc oxide nanoparticles into the viable epidermis of human skin in vivo. Eur J Pharm Biopharm 2013;84:297-308.
10. Creutzenberg O, Bellmann B, Korolewitz R, et al. Change in agglomeration status and toxicokinetic fate of various nanoparticles in vivo following lung exposure in rats. Inhal Toxicol 2012;24:821-30.
11. van der Zande M, Vandebriel RJ, Van Doren E, et al. Distribution, elimination, and toxicity of silver nanoparticles and silver ions in rats after 28-day oral exposure. ACS Nano 2012;6:7427-42.
12. Yamashita K, Yoshioka Y, Higashisaka K, et al. Silica and titanium dioxide nanoparticles cause pregnancy complications in mice. Nat Nanotechnol 2011;6:321-8.
13. Huang JP, Hsieh PC, Chen CY, et al. Nanoparticles can cross mouse placenta and induce trophoblast apoptosis. Placenta 2015;36:1433-41.
14. Shirasuna K, Usui F, Karasawa T, et al. Nanosilica-induced placental inflammation and pregnancy complications: Different roles of the inflammasome components NLRP3 and ASC. Nanotoxicology 2015;9:554-67.
15. Campagnolo L, Massimiani M, Palmieri G, et al. Biodistribution and toxicity of pegylated single wall carbon nanotubes in pregnant mice. Part Fibre Toxicol 2013;10:21.
16. Onoda A, Takeda K, Umezawa M. Dose-dependent induction of astrocyte activation and reactive astrogliosis in mouse brain following maternal exposure to carbon black nanoparticle. Part Fibre Toxicol 2017;14:4.
17. Park EJ, Choi J, Park YK, et al. Oxidative stress induced by cerium oxide nanoparticles in cultured BEAS-2B cells. Toxicology 2008;245:90-100.
18. Thill A, Zeyons O, Spalla O, et al. Cytotoxicity of CeO2 nanoparticles for Escherichia coli. Physico-chemical insight of the cytotoxicity mechanism. Environ Sci Technol 2006;40:6151-6.
19. Hussain S, Al-Nsour F, Rice AB, et al. Cerium dioxide nanoparticles induce apoptosis and autophagy in human peripheral blood monocytes. ACS Nano 2012;6:5820-9.
20. Falchi L, Bogliolo L, Galleri G, et al. Cerium dioxide nanoparticles did not alter the functional and morphologic characteristics of ram sperm during short-term exposure. Theriogenology 2016;85:1274-81.e3.
21. Qin F, Shen T, Li J, et al. SF-1 mediates reproductive toxicity induced by Cerium oxide nanoparticles in male mice. J Nanobiotechnology 2019;17:41.
22. Ariu F, Bogliolo L, Pinna A, et al. Cerium oxide nanoparticles (CeO2 NPs) improve the developmental competence of in vitro-matured prepubertal ovine oocytes. Reprod Fertil Dev 2017;29:1046-56.
23. Graham CH, Hawley TS, Hawley RG, et al. Establishment and characterization of first trimester human trophoblast cells with extended lifespan. Exp Cell Res 1993;206:204-11.
24. Winship A, Cuman C, Rainczuk K, et al. Fibulin-5 is upregulated in decidualized human endometrial stromal cells and promotes primary human extravillous trophoblast outgrowth. Placenta 2015;36:1405-11.
25. Bone CR, Chang YT, Cain NE, et al. Nuclei migrate through constricted spaces using microtubule motors and actin networks in C. elegans hypodermal cells. Development 2016;143:4193-202.
26. Hamutoğlu R, Bulut HE, Kaloğlu C, et al. The regulation of trophoblast invasion and decidual reaction by matrix metalloproteinase-2, metalloproteinase-7, and metalloproteinase-9 expressions in the rat endometrium.

Reprod Med Biol 2020;19:385-97.
27. Xu P, Alfaidy N, Challis JR. Expression of matrix metalloproteinase (MMP)-2 and MMP-9 in human placenta and fetal membranes in relation to preterm and term labor. J Clin Endocrinol Metab 2002;87:1353-61.
28. Buck E, Eyzaguirre A, Brown E, et al. Rapamycin synergizes with the epidermal growth factor receptor inhibitor erlotinib in non-small-cell lung, pancreatic, colon, and breast tumors. Mol Cancer Ther 2006;5:2676-84.
29. Dennis PB, Jaeschke A, Saitoh M, et al. Mammalian TOR: a homeostatic ATP sensor. Science 2001;294:1102-5.
30. Dudkin L, Dilling MB, Cheshire PJ, et al. Biochemical correlates of mTOR inhibition by the rapamycin ester CCI-779 and tumor growth inhibition. Clin Cancer Res 2001;7:1758-64.
31. Knöfler M. Critical growth factors and signalling pathways controlling human trophoblast invasion. Int J Dev Biol 2010;54:269-80.
32. Bischof P, Meisser A, Campana A. Paracrine and autocrine regulators of trophoblast invasion--a review. Placenta 2000;21 Suppl A:S55-60.
33. Strickland S, Richards WG. Invasion of the trophoblasts. Cell 1992;71:355-7.
34. Xue HY, Liu Y, Liao JZ, et al. Gold nanoparticles delivered miR-375 for treatment of hepatocellular carcinoma. Oncotarget 2016;7:86675-86.
35. Tran TA, Krishnamoorthy K, Cho SK, et al. Inhibitory Effect of Zinc Sulfide Nanoparticles Towards Breast Cancer Stem Cell Migration and Invasion. J Biomed Nanotechnol 2016;12:329-36.
36. Seval Y, Akkoyunlu G, Demir R, et al. Distribution patterns of matrix metalloproteinase (MMP)-2 and -9 and their inhibitors (TIMP-1 and TIMP-2) in the human decidua during early pregnancy. Acta Histochem 2004;106:353-62.
37. Zhu JY, Pang ZJ, Yu YH. Regulation of trophoblast invasion: the role of matrix metalloproteinases. Rev Obstet Gynecol 2012;5:e137-43.
38. Sonderegger S, Haslinger P, Sabri A, et al. Wingless (Wnt)-3A induces trophoblast migration and matrix metalloproteinase-2 secretion through canonical Wnt signaling and protein kinase B/AKT activation. Endocrinology 2010;151:211-20.
39. Jia RZ, Rui C, Li JY, et al. CDX1 restricts the invasion of HTR-8/SVneo trophoblast cells by inhibiting MMP-9 expression. Placenta 2014;35:450-4.
40. Si X, Xu F, Xu F, et al. CADM1 inhibits ovarian cancer cell proliferation and migration by potentially regulating the PI3K/Akt/mTOR pathway. Biomed Pharmacother 2020;123:109717.
41. Doridot L, Miralles F, Barbaux S, et al. Trophoblasts, invasion, and microRNA. Front Genet 2013;4:248.
42. Yu Y, Wang L, Liu T, et al. MicroRNA-204 suppresses trophoblast-like cell invasion by targeting matrix metalloproteinase-9. Biochem Biophys Res Commun 2015;463:285-91.
43. Li P, Guo W, Du L, et al. microRNA-29b contributes to pre-eclampsia through its effects on apoptosis, invasion and angiogenesis of trophoblast cells. Clin Sci (Lond) 2013;124:27-40.
44. Zhong W, Peng H, Tian A, et al. Expression of miRNA-1233 in placenta from patients with hypertensive disorder complicating pregnancy and its role in disease pathogenesis. Int J Clin Exp Med 2015;8:9121-7.
45. Chen Z, Jin Y, Yu D, et al. Down-regulation of the microRNA-99 family members in head and neck squamous cell carcinoma. Oral Oncol 2012;48:686-91.
46. Sun D, Lee YS, Malhotra A, et al. miR-99 family of MicroRNAs suppresses the expression of prostate-specific antigen and prostate cancer cell proliferation. Cancer Res 2011;71:1313-24.
47. Li BH, Zhou JS, Ye F, et al. Reduced miR-100 expression in cervical cancer and precursors and its carcinogenic effect through targeting PLK1 protein. Eur J Cancer 2011;47:2166-74.

(English Language Editor: K. Brown)

Cite this article as: Yao M, Ji X, Zhang Y, Mao Z, Chi X. miR-99 family is potential target to reverse cerium dioxide nanoparticle-induced placental cell dysfunction. Ann Transl Med 2022;10(7):402. doi: 10.21037/atm-22-508